Hindawi Publishing Corporation
Mathematical Problems in Engineering
Volume 2015, Article ID 637254, 10 pages
http://dx.doi.org/10.1155/2015/637254

Research Article

Mode Stresses for the Interaction between an Inclined Crack and a Curved Crack in Plane Elasticity

N. M. A. Nik Long,[1,2] M. R. Aridi,[2,3] and Z. K. Eshkuvatov[2,4]

[1] *Mathematics Department, Faculty of Science, Universiti Putra Malaysia, 43400 Serdang, Selangor, Malaysia*
[2] *Institute for Mathematical Research, Universiti Putra Malaysia, 43400 Serdang, Selangor, Malaysia*
[3] *College of Foundation and General Studies, Universiti Tenaga Nasional, 43000 Kajang, Selangor, Malaysia*
[4] *Faculty of Science and Technology, Universiti Sains Islam Malaysia (USIM), 71800 Negeri Sembilan, Malaysia*

Correspondence should be addressed to N. M. A. Nik Long; nmasri@upm.edu.my

Received 22 September 2014; Accepted 8 December 2014

Academic Editor: Trung Nguyen-Thoi

The interaction between the inclined and curved cracks is studied. Using the complex variable function method, the formulation in hypersingular integral equations is obtained. The curved length coordinate method and suitable quadrature rule are used to solve the integral equations numerically for the unknown function, which are later used to evaluate the stress intensity factor. There are four cases of the mode stresses; Mode I, Mode II, Mode III, and Mix Mode are presented as the numerical examples.

1. Introduction

For two-dimensional crack, Panasyuk et al. [1], Cotterell and Rice [2], Shen [3], and Martin [4] used perturbation method to obtain the elastic stress intensity factor for a variety of crack positions. Formulation in terms of singular, hypersingular, or Fredholm integral equations for solving single [5] and multiple cracks problems [6] in various sets of cracks positions was proposed later. These integral equations are solved numerically. Numerical solution of the curved crack problem using polynomial approximation of the dislocation distribution was achieved by taking the crack opening displacement (COD) as the unknown and the resultant forces as the right term in the equations [7].

The curved length coordinate method [8] where the crack is mapped on a real axis provides an effective way to solve the integral equations for the curved crack. Boundary element method, which avoids singularities of the resulting algebraic system of equation [9], and the dual boundary element method [10] have also been considered successfully.

In this paper, the interaction between inclined and curved cracks is formulated into the hypersingular integral equations using the complex potential method. This approach has been considered by Guo and Lu [11]. Then, by the curved length coordinate method, the cracks are mapped into a straight line, which require less collocation points, and hence give faster convergence. In order to solve the equations numerically, the quadrature rules are applied and we obtained a system of algebraic equations for solving the unknown coefficients. The obtained unknown coefficients will later be used in calculating the SIF.

2. Complex Variable Function Method

The complex variable function method is used to formulate the hypersingular integral equation for the interaction between an inclined crack and a curved crack. Let $\Phi(z) = \phi'(z)$ and $\Psi(z) = \psi'(z)$ be two complex potentials. Then the stress $(\sigma_x, \sigma_y, \sigma_z)$, the resultant function (X, Y), and the displacement (u, v) are related to $\Phi(z)$ and $\Psi(z)$ as [12]

$$\sigma_x + \sigma_y = 4\,\mathrm{Re}\,\Phi(z), \tag{1}$$

$$\sigma_y - \sigma_x + 2i\sigma_{xy} = 2\left[\overline{z}\Phi'(z) + \Psi(z)\right], \tag{2}$$

$$f = -Y + iX = \phi(z) + z\overline{\phi'(z)} + \overline{\psi(z)} + c, \tag{3}$$

$$2G(u + iv) = K\phi(z) - z\overline{\phi'(z)} + \psi(z), \tag{4}$$

where G is shear modulus of elasticity, $K = 3 - \nu$ for plane strain, and $K = (3 - \nu)/(1 + \nu)$ for plane stress; ν is Poisson's ratio and $z = x + iy$. The derivative in a specified direction (DISD) is defined as

$$J\left(z, \bar{z}, \frac{d\bar{z}}{dz}\right) = \frac{d}{dz}\{-Y + iX\} = \Phi(z) + \overline{\Phi(z)} + \frac{d\bar{z}}{dz}\left(z\overline{\Phi'(z)} + \overline{\Psi(z)}\right) = N + iT, \tag{5}$$

where J denotes the normal and tangential tractions along the segment $\overline{z, z + dt}$. Note that the value of J depends not only on the position of point z, but also on the direction of the segment $d\bar{z}/dz$ [5].

The complex potential in plane elasticity is obtained by placing two point dislocations with intensities H and $-H$ at points $z = t$ and $z = t + dt$, yielding

$$\phi(z) = -H\frac{dt}{z - t}, \qquad \psi(z) = -\overline{H}\frac{dt}{z - t} - H\frac{d\bar{t}}{t - z} + H\frac{\bar{t}dt}{(t - z)^2}. \tag{6}$$

Making substitutions H and $\overline{H}$ by $-g(t)/2\pi$ and $-\overline{g(t)}/2\pi$ in (6) and performing integration on the right side of (6) give

$$\phi(z) = \frac{1}{2\pi}\int_L \frac{g(t)\,dt}{t - z}, \qquad \psi(z) = \frac{1}{2\pi}\left[\int_L \frac{g(t)\,d\bar{t}}{t - z} + \int_L \frac{\overline{g(t)}dt}{t - z} - \int_L \frac{\bar{t}g(t)\,dt}{(t - z)^2}\right], \tag{7}$$

where L denotes the crack configuration. Substituting (7) into (4) and letting z approach t_0^+ and t_0^-, which are located on the upper and lower sides of the crack faces, then using the Plemelj equations, and rewriting t_0 as t, the following result is obtained [5]:

$$2G(u(t) + iv(t)) = i(k + 1)\,g(t), \quad (t \in L), \tag{8}$$

where $(u(t) + iv(t)) = (u(t) + iv(t))^+ - (u(t) + iv(t))^-$ denotes the crack opening displacement (COD) for both cracks. It is well known that the COD possesses the following properties:

$$g(t) = O\left[\left(t - t_{B_1}\right)^{1/2}\right] \text{ at the crack tip } B_1, \qquad g(t) = O\left[\left(t - t_{B_2}\right)^{1/2}\right] \text{ at the crack tip } B_2. \tag{9}$$

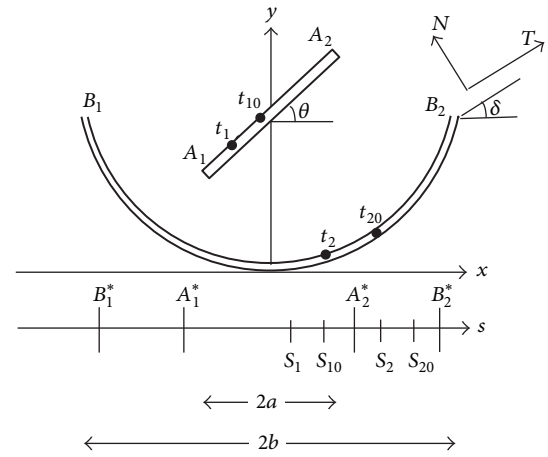

Figure 1: Inclined and curved cracks in plane elasticity with configurations on a real axis s. Cracks with lengths $2a$ (inclined) and $2b$ (curved) are known as crack-1 and crack-2, respectively.

3. Hypersingular Integral Equation

The hypersingular integral equation for an inclined or a curved crack problem is obtained by placing two point dislocations at points $z = t$ and $z = t + dt$. It is given by [5]

$$\frac{1}{\pi}\text{h.p.}\int_L \frac{g(t)\,dt}{(t - t_0)^2} + \frac{1}{2\pi}\int_L K_1(t, t_0)\,g(t)\,dt + \frac{1}{2\pi}\int_L K_2(t, t_0)\,\overline{g(t)}dt = N(t_0) + iT(t_0), \quad t_0 \in L, \tag{10}$$

where

$$K_1(t, t_0) = \frac{-1}{(t - t_0)^2} + \frac{1}{(\bar{t} - \bar{t}_0)^2}\frac{d\bar{t}_0}{dt_0}\frac{d\bar{t}}{dt}, \qquad K_2(t, t_0) = \frac{-1}{(\bar{t} - \bar{t}_0)^2}\left(\frac{d\bar{t}}{dt} + \frac{d\bar{t}_0}{dt_0}\right) - \frac{2(t - t_0)}{(\bar{t} - \bar{t}_0)^3}\frac{d\bar{t}_0}{dt_0}\frac{d\bar{t}}{dt} \tag{11}$$

and $g(t)$ is the dislocation distribution along the curved crack. In (10), the first integral with h.p. denotes the hypersingular integral and it must be interpreted in Hadamart sense [8].

Now consider the interaction between inclined and curved cracks problem (see Figure 1). For the crack-1, if the point dislocation is placed at points $z = t_{10}$ and $z = dt_{10}$, $g_1(t_1)$ is the dislocation doublet distribution along crack-1, and the traction is applied on the t_{10}, then the hypersingular integral equation for crack-1 is

$$\frac{1}{\pi}\text{h.p.}\int_{L_1} \frac{g_1(t_1)\,dt_1}{(t_1 - t_{10})^2} + \frac{1}{2\pi}\int_{L_1} K_1(t_1, t_{10})\,g_1(t_1)\,dt_1 + \frac{1}{2\pi}\int_{L_1} K_2(t_1, t_{10})\,\overline{g_1(t_1)}dt_1 = N_{11}(t_{10}) + iT_{11}(t_{10}), \tag{12}$$

where $N_{11}(t_{10}) + iT_{11}(t_{10})$ denotes the traction influence on crack-1 caused by dislocation doublet distribution, $g_1(t_1)$, on crack-1 and

$$K_1(t_1, t_{10}) = \frac{-1}{(t_1 - t_{10})^2} + \frac{1}{(\bar{t}_1 - \bar{t}_{10})^2} \frac{d\bar{t}_{10}}{dt_{10}} \frac{d\bar{t}_1}{dt_1},$$

$$K_2(t_1, t_{10}) = \frac{-1}{(\bar{t}_1 - \bar{t}_{10})^2} \left(\frac{d\bar{t}_1}{dt_1} + \frac{d\bar{t}_{10}}{dt_{10}} \right) - \frac{2(t_1 - t_{10})}{(\bar{t}_1 - \bar{t}_{10})^3} \frac{d\bar{t}_{10}}{dt_{10}} \frac{d\bar{t}_1}{dt_1}. \tag{13}$$

The influence from the dislocation doublet distribution on crack-2 gives

$$\frac{1}{\pi} \int_{L_2} \frac{g_2(t_2)\, dt_2}{(t_2 - t_{10})^2} + \frac{1}{2\pi} \int_{L_2} K_1(t_2, t_{10})\, g_2(t_2)\, dt_2 + \frac{1}{2\pi} \int_{L_2} K_2(t_2, t_{10}) \overline{g_2(t_2)} dt_2 = N_{12}(t_{10}) + iT_{12}(t_{10}), \tag{14}$$

where $N_{12}(t_{10}) + iT_{12}(t_{10})$ denotes the traction influence on crack-1 caused by dislocation doublet distribution, $g_2(t_2)$, on crack-2 and

$$K_1(t_2, t_{10}) = \frac{-1}{(t_2 - t_{10})^2} + \frac{1}{(\bar{t}_2 - \bar{t}_{10})^2} \frac{d\bar{t}_{10}}{dt_{10}} \frac{d\bar{t}_2}{dt_2},$$

$$K_2(t_2, t_{10}) = \frac{-1}{(\bar{t}_2 - \bar{t}_{10})^2} \left(\frac{d\bar{t}_2}{dt_2} + \frac{d\bar{t}_{10}}{dt_{10}} \right) - \frac{2(t_2 - t_{10})}{(\bar{t}_2 - \bar{t}_{10})^3} \frac{d\bar{t}_{10}}{dt_{10}} \frac{d\bar{t}_2}{dt_2}. \tag{15}$$

Note that since $t_2 - t_{10} \neq 0$, all three integrals in (14) are regular and note that $g_1(t_1)$ and $g_2(t_2)$ satisfy (9). By superposition of the dislocation doublet distribution, $g_1(t_1)$, along crack-1 (12) and the dislocation doublet distribution, $g_2(t_2)$, along crack-2 (14), we obtained the following hypersingular integral equation for crack-1 which is as follows:

$$\frac{1}{\pi} \text{h.p.} \int_{L_1} \frac{g_1(t_1)\, dt_1}{(t_1 - t_{10})^2} + \frac{1}{2\pi} \int_{L_1} K_1(t_1, t_{10})\, g_1(t_1)\, dt_1 + \frac{1}{2\pi} \int_{L_1} K_2(t_1, t_{10}) \overline{g_1(t_1)} dt_1 + \frac{1}{\pi} \int_{L_2} \frac{g_2(t_2)\, dt_2}{(t_2 - t_{10})^2} + \frac{1}{2\pi} \left[\int_{L_2} \left(K_1(t_2, t_{10})\, g_2(t_2) + K_2(t_2, t_{10}) \overline{g_2(t_2)} \right) dt_2 \right] = N_1(t_{10}) + iT_1(t_{10}), \tag{16}$$

where $N_1(t_{10}) + iT_1(t_{10}) = N_{11}(t_{10}) + N_{12}(t_{10}) + i(T_{11}(t_{10}) + iT_{12}(t_{10}))$ is the traction applied at point t_{10} of crack-1, which is derived from the boundary condition. The first three integrals in (16) represent the effect on crack-1 caused by the dislocation on crack-1 itself, whereas the second three integrals represent the effect of the dislocations on crack-2.

Similarly, the hypersingular integral equation for crack-2 is

$$\frac{1}{\pi} \text{h.p.} \int_{L_2} \frac{g_2(t_2)\, dt_2}{(t_2 - t_{20})^2} + \frac{1}{2\pi} \int_{L_2} K_1(t_2, t_{20})\, g_2(t_2)\, dt_2 + \frac{1}{2\pi} \int_{L_2} K_2(t_2, t_{20}) \overline{g_2(t_2)} dt_2 + \frac{1}{\pi} \int_{L_1} \frac{g_1(t_1)\, dt_1}{(t_1 - t_{20})^2} + \frac{1}{2\pi} \left[\int_{L_1} \left(K_1(t_1, t_{20})\, g_1(t_1) + K_2(t_1, t_{20}) \overline{g_1(t_1)} \right) dt_1 \right] = N_2(t_{20}) + iT_2(t_{20}), \tag{17}$$

where $N_2(t_{20}) + iT_2(t_{20}) = N_{21}(t_{20}) + N_{22}(t_{20}) + i(T_{21}(t_{20}) + iT_{22}(t_{20}))$ is the traction applied at point t_{20} of crack-2 and

$$K_1(t_2, t_{20}) = \frac{-1}{(t_2 - t_{20})^2} + \frac{1}{(\bar{t}_2 - \bar{t}_{20})^2} \frac{d\bar{t}_{20}}{dt_{20}} \frac{d\bar{t}_2}{dt_2},$$

$$K_2(t_2, t_{20}) = \frac{-1}{(\bar{t}_2 - \bar{t}_{20})^2} \left(\frac{d\bar{t}_2}{dt_2} + \frac{d\bar{t}_{20}}{dt_{20}} \right) - \frac{2(t_2 - t_{20})}{(\bar{t}_2 - \bar{t}_{20})^3} \frac{d\bar{t}_{20}}{dt_{20}} \frac{d\bar{t}_2}{dt_2},$$

$$K_1(t_1, t_{20}) = \frac{-1}{(t_1 - t_{20})^2} + \frac{1}{(\bar{t}_1 - \bar{t}_{20})^2} \frac{d\bar{t}_{20}}{dt_{20}} \frac{d\bar{t}_1}{dt_1},$$

$$K_2(t_1, t_{20}) = \frac{-1}{(\bar{t}_1 - \bar{t}_{20})^2} \left(\frac{d\bar{t}_1}{dt_1} + \frac{d\bar{t}_{20}}{dt_{20}} \right) - \frac{2(t_1 - t_{20})}{(\bar{t}_1 - \bar{t}_{20})^3} \frac{d\bar{t}_{20}}{dt_{20}} \frac{d\bar{t}_1}{dt_1}. \tag{18}$$

In (17), the first three integrals represent the effect on crack-2 caused by the dislocation on crack-2 itself, and the second three integrals represent the effect of the dislocation on crack-1. Equations (16) and (17) are to be solved for $g_1(t_1)$ and $g_2(t_2)$.

Mapping the two cracks configurations on a real axis s with intervals $2a$ and $2b$, respectively, the mapping functions $t_1(s_1)$ and $t_2(s_2)$ are expressed as

$$g_1(t_1)\big|_{t_1 = t_1(s_1)} = \sqrt{a^2 - s_1^2} H_1(s_1), \tag{19}$$

$$g_2(t_2)\big|_{t_2 = t_2(s_2)} = \sqrt{b^2 - s_2^2} H_2(s_2), \tag{20}$$

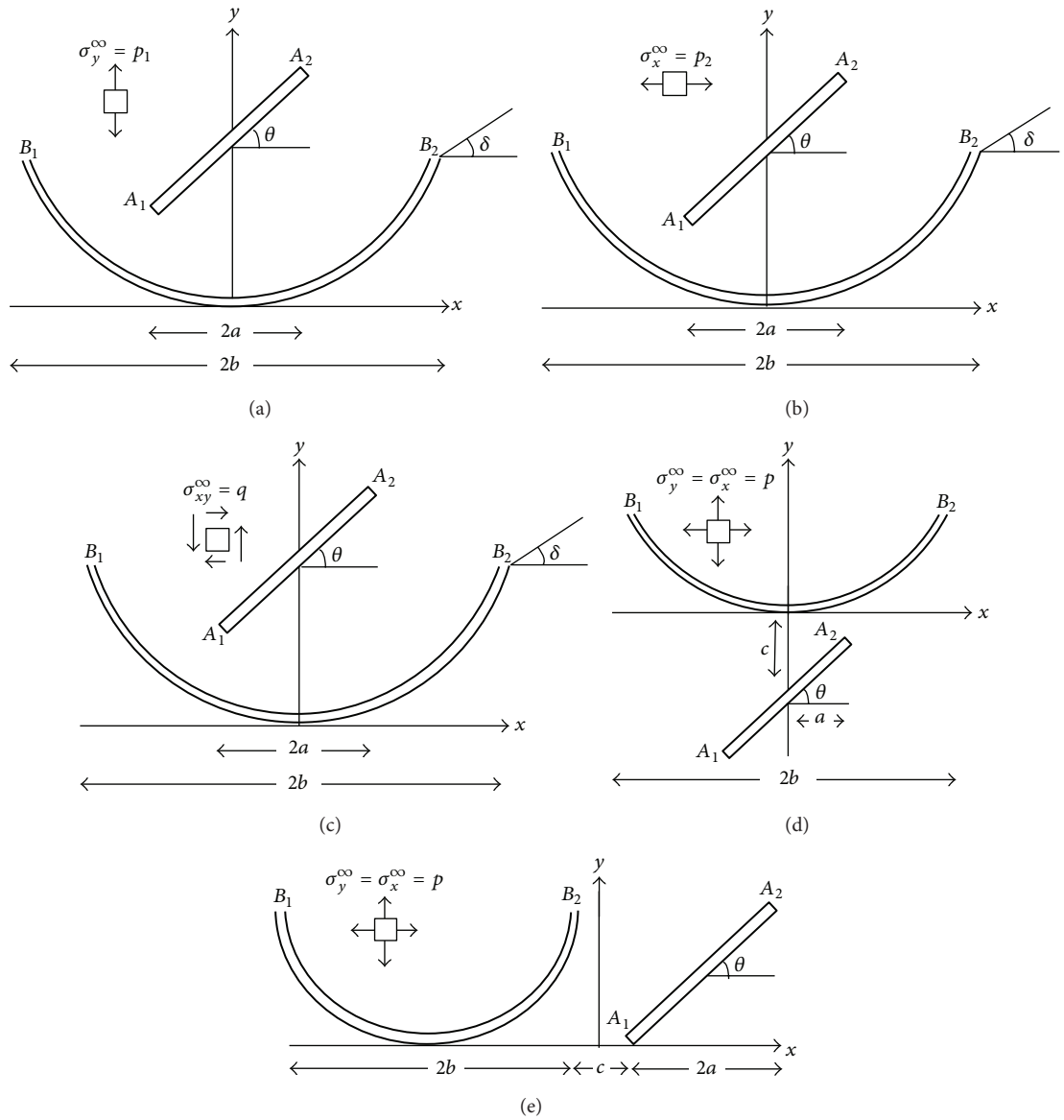

Figure 2: (a) An inclined crack in upper position of a curved crack (Mode I). (b) An inclined crack in upper position of a curved crack (Mode II). (c) An inclined crack in upper position of a curved crack (Mode III). (d) An inclined crack is located below the curved crack (Mix Mode). (e) An inclined crack is located on the right position of the curved crack (Mix Mode).

where $H_1(s_1) = H_{11}(s_1) + iH_{12}(s_1)$ and $H_2(s_2) = H_{21}(s_2) + iH_{22}(s_2)$. In solving the integral equations, we used the following integration rules [13] for the hypersingular and regular integrals, respectively;

$$\frac{1}{\pi}\text{h.p.}\int_{-a}^{a}\frac{\sqrt{a^2-s^2}G(s)}{(s-s_0)^2}ds=\sum_{j=1}^{M+1}W_j(s_0)\,G(s_j),\quad(|s_0|<a),\tag{21}$$

$$\frac{1}{\pi}\int_{-a}^{a}\sqrt{a^2-s^2}G(s)\,ds=\frac{1}{M+2}\sum_{j=1}^{M+1}\left(a^2-s_j^{\,2}\right)G(s_j),\quad(|s_0|<a),\tag{22}$$

where $G(s)$ is a given regular function, $M\in\mathbb{Z}$,

$$s_j=s_{0j}=a\cos\left(\frac{j\pi}{M+2}\right),\quad j=1,2,3,\ldots,M+1,$$
$$W_j(s_0)=-\frac{2}{M+2}\sum_{n=0}^{M}(n+1)\,V_j^nU_n\left(\frac{s_0}{a}\right),\tag{23}$$

where

$$V_j^n=\sin\left(\frac{j\pi}{M+2}\right)\sin\left(\frac{(n+1)\,j\pi}{M+2}\right).\tag{24}$$

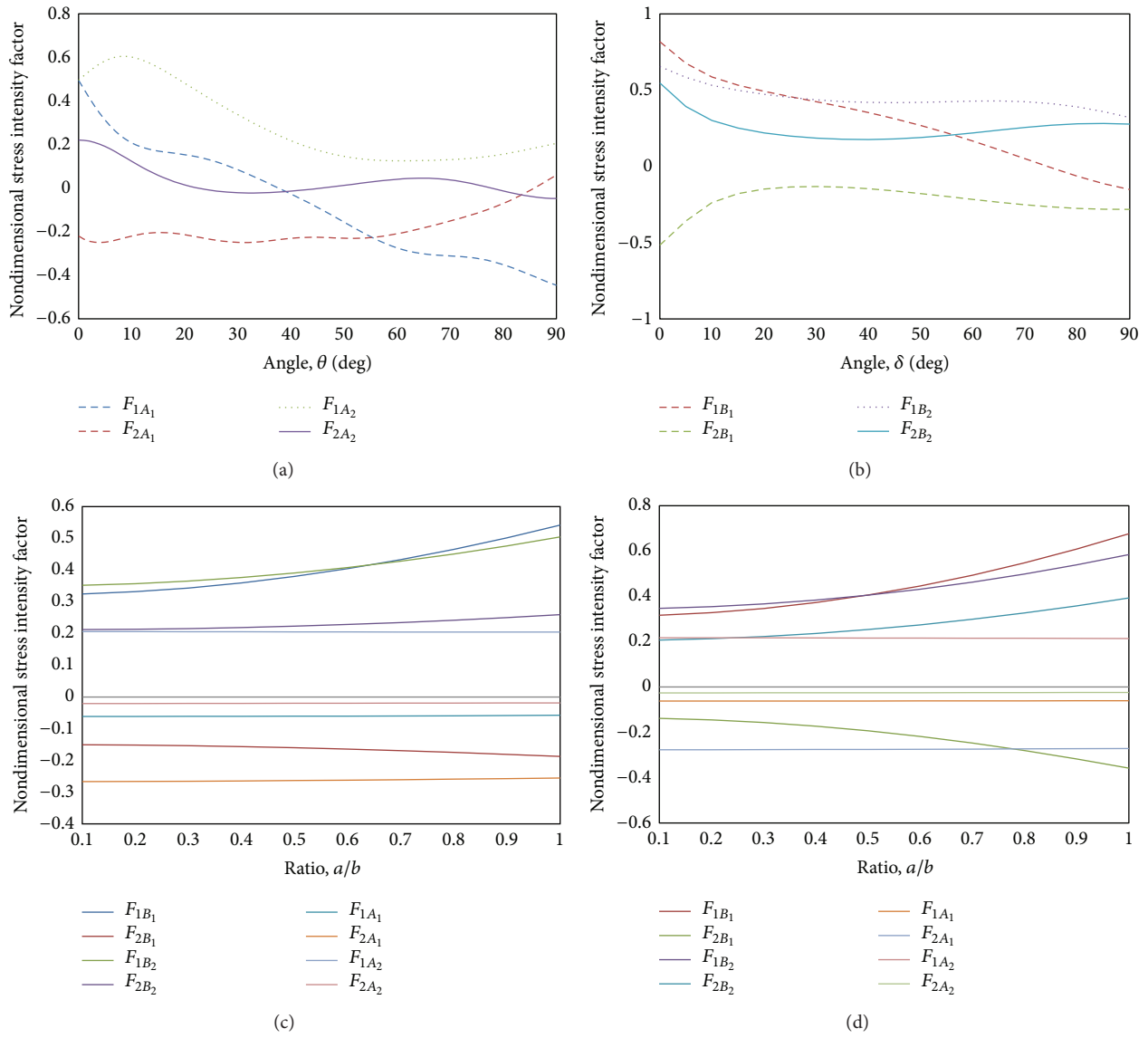

Figure 3: Nondimensional SIF for the interaction between an inclined and a curved crack subject to normal loading (Mode I) (see Figure 2(a)).

Here $U_n(t)$ is a Chebyshev polynomial of the second kind, defined by

$$U_n(t) = \sin\left(\frac{(n+1)\theta}{\sin\theta}\right), \quad t = \cos\theta. \tag{25}$$

$H_1(s)$ and $H_2(s)$ can be evaluated using

$$H_1(s) = \sum_{n=0}^{M} c_{1n} U_n\left(\frac{s}{a}\right), \quad |s_0| < a,$$
$$H_2(s) = \sum_{n=0}^{M} c_{2n} U_n\left(\frac{s}{b}\right), \quad |s_0| < b, \tag{26}$$

where

$$c_{1n} = \frac{2}{M+2} \sum_{j=1}^{M+1} V_j^n H_1(s_1),$$
$$c_{2n} = \frac{2}{M+2} \sum_{j=1}^{M+1} V_j^n H_2(s_2), \tag{27}$$

and $H_1(s_1)$ and $H_1(s_2)$ are defined from (19) and (20), respectively.

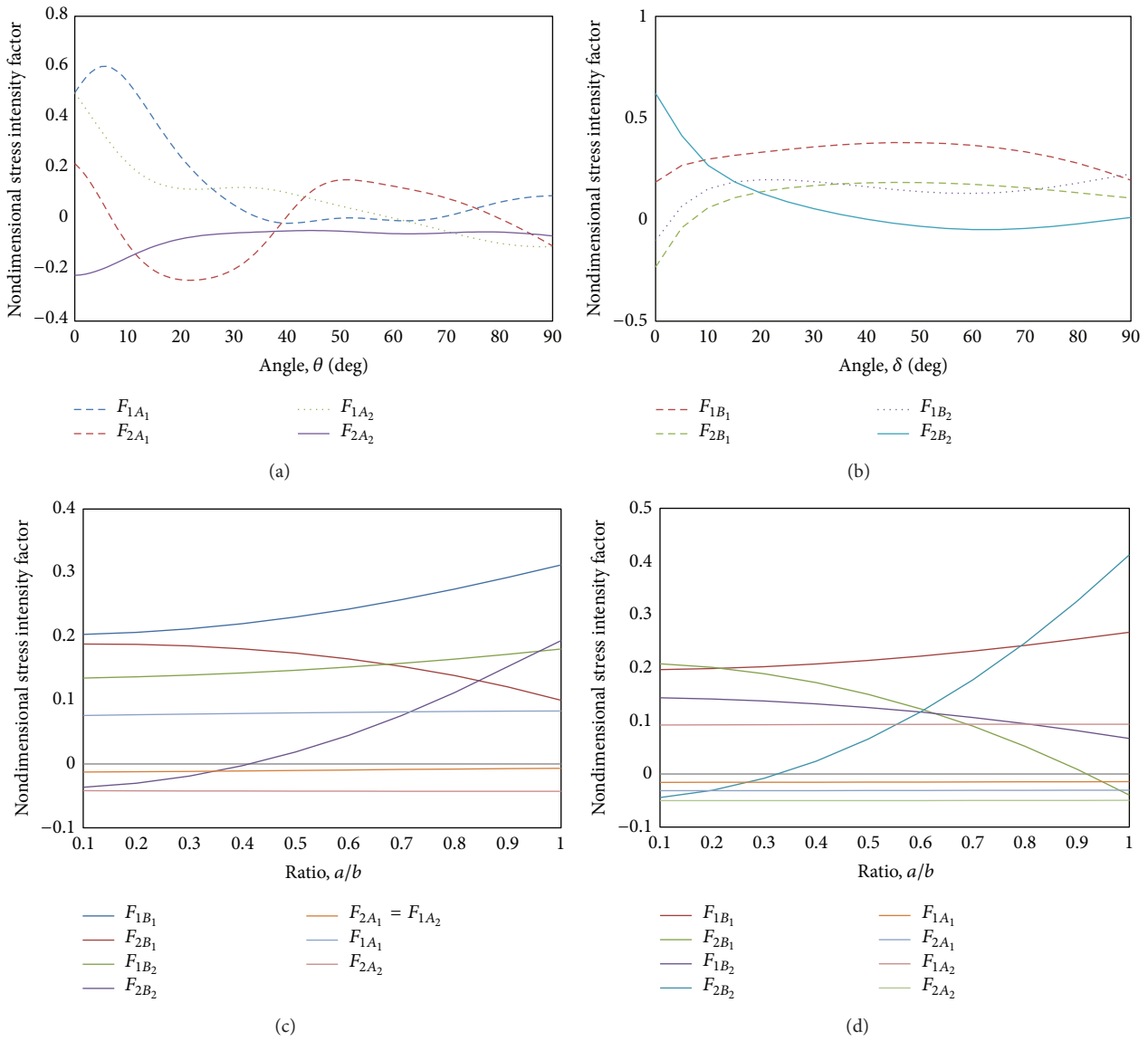

FIGURE 4: Nondimensional SIF for the interaction between an inclined and a curved crack subject to shear loading (Mode II) (see Figure 2(b)).

4. Stress Intensity Factor

The stress intensity factor (SIF) for the two cracks can be calculated, respectively, as follows:

$$K_{A_j} = (K_1 - iK_2)_{A_j} = \sqrt{2\pi} \lim_{t \to t_{A_j}} \sqrt{\left|t - t_{A_j}\right|} g_1'(t), \quad j = 1, 2,$$
$$K_{B_j} = (K_1 - iK_2)_{B_j} = \sqrt{2\pi} \lim_{t \to t_{B_j}} \sqrt{\left|t - t_{B_j}\right|} g_2'(t), \quad j = 1, 2, \tag{28}$$

where $g_1'(t)$ and $g_2'(t)$ are obtained by solving (19) and (20), simultaneously.

In order to show that the suggested method can be used for solving more complicated curved cracks problems, several numerical examples are presented. For verification purposes, we observe that if the two cracks are far apart, we have $|t_2 - t_{10}|$ and $|t_1 - t_{20}|$ approach infinity. These lead to the second three integrals vanish in (16) and (17). Then (16) and (17) become an equation for an inclined and a curved crack, respectively. For the curved crack with the length $2b$, we compare the result with the exact solution with the remote traction $\sigma_x^\infty = \sigma_y^\infty = 1$, given by Cotterell and Rice [2]:

$$K_1 = \frac{(\pi b)^{1/2} \cos(\delta/2)}{1 + \sin^2(\delta/2)}, \qquad K_2 = \frac{(\pi b)^{1/2} \sin(\delta/2)}{1 + \sin^2(\delta/2)}, \tag{29}$$

where δ is the tangent angle at the direction of crack tip.

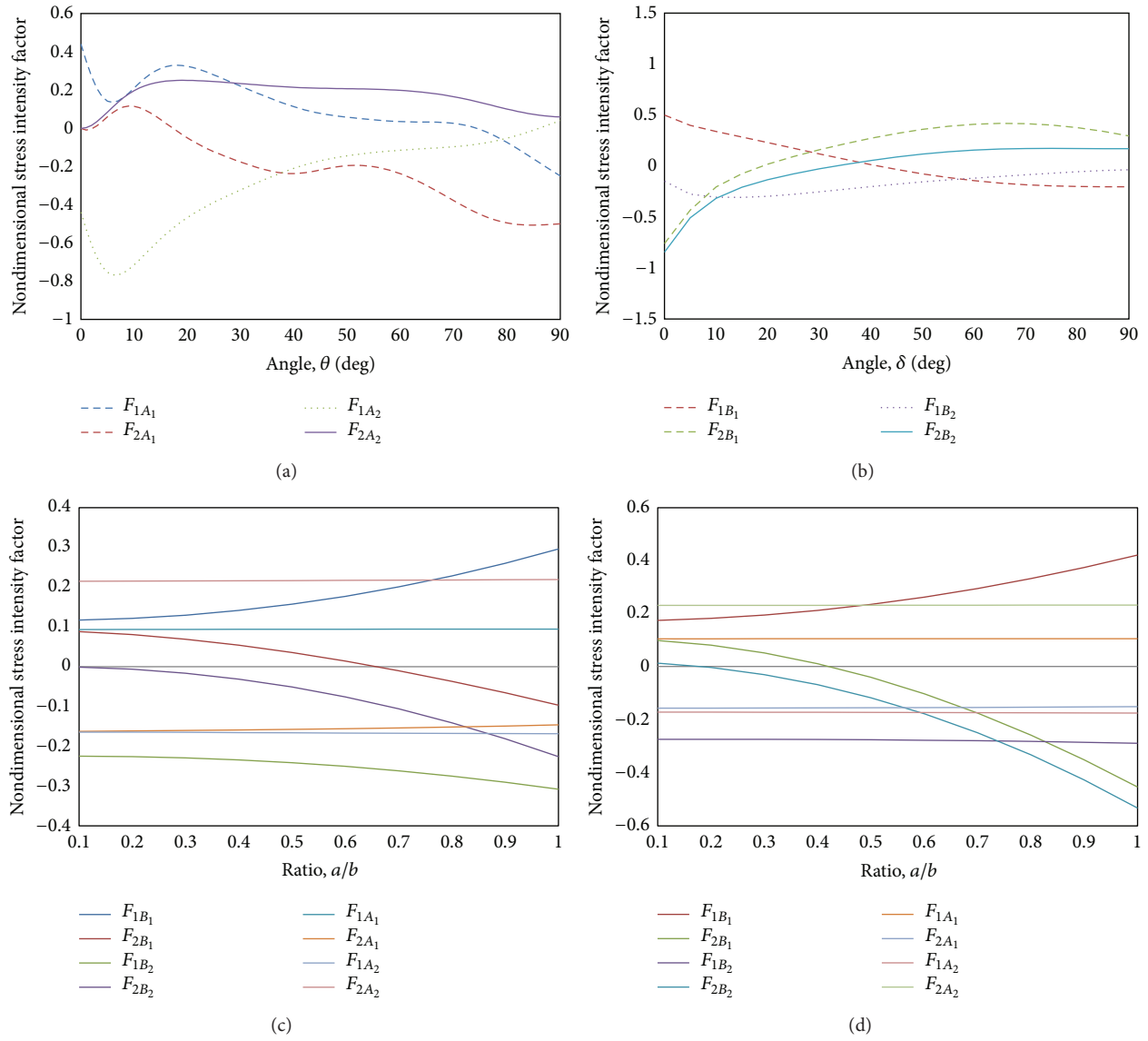

Figure 5: Nondimensional SIF for the interaction between an inclined and a curved crack subject to tearing loading (Mode III) (see Figure 2(c)).

Table 1: The SIF for single curved crack: a comparison between exact and numerical results.

θ	K_{1A_1}	K_{1A_1} (exact)	K_{2A_1}	K_{2A_1} (exact)
15	0.9980	0.9989	0.0174	0.0174
30	0.9956	0.9967	0.0466	0.0465
45	0.9913	0.9927	0.0694	0.0693
60	0.9826	0.9871	0.0928	0.0924
75	0.9714	0.9748	0.1117	0.1145
90	0.9611	0.9713	0.1382	0.1369

The numerical results are tabulated in Table 1. It can be seen that maximum error is less than 1.0%.

4.1. Example 1: Mode I. Consider an inclined crack in upper position of a curved crack (Figure 2(a)); the traction applied is $\sigma_y^{\infty} = p_1$ and the calculated results for SIF at the crack tips A_1, A_2, B_1, and B_2 are, respectively, expressed as

$$K_{iA_j} = F_{iA_j}\left(\frac{a}{b}, \theta\right) p_1 \sqrt{\pi a}, \quad i, j = 1, 2,$$
$$K_{iB_j} = F_{iB_j}\left(\frac{a}{b}, \delta\right) p_1 \sqrt{\pi b}, \quad i, j = 1, 2. \tag{30}$$

Figure 3(a) shows the nondimensional SIF for an inclined crack when θ is changing for $\delta = 45^{\circ}$. It can be seen that as θ

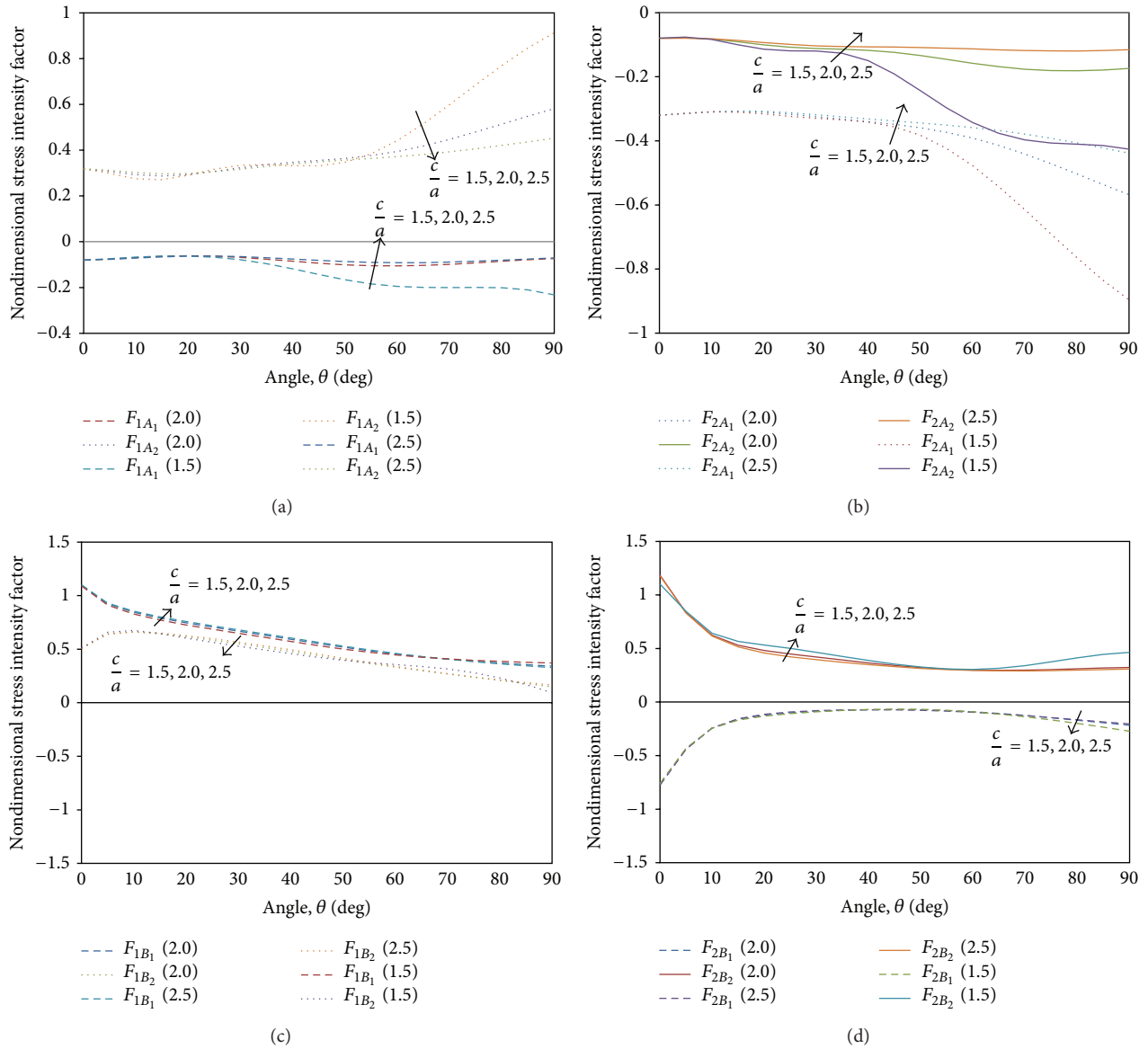

Figure 6: Nondimensional SIF at the crack tips when θ is changing subject to mix loading (see Figure 2(d)).

varies within the range $0^\circ \le \delta \le 90^\circ$, the values of F_{1A_1}, F_{2A_1}, F_{1A_2}, and F_{2A_2} are varied significantly due to shielding effect. Whereas Figure 3(b) shows the nondimensional SIF for a curved crack when δ is changing for $\theta = 45^\circ$, the values of F_{1B_1}, F_{2B_1}, F_{1B_2}, and F_{2B_2} are varied significantly for the considered domain.

The effect of the distance between both cracks, a/b, is also studied by taking $\theta = 45^\circ$ and the results are shown in Figures 3(c) and 3(d) for $\delta = 90^\circ$ and $\delta = 45^\circ$, respectively. As the two cracks are close together, the nondimensional SIF at the crack tip becomes higher.

4.2. Example 2: Mode II. Consider the problem in Figure 2(b); the traction applied is $\sigma_x^\infty = p_2$ and the calculated results for SIF at the crack tips A_1, A_2, B_1, and B_2 are, respectively, expressed as

$$K_{iA_j} = F_{iA_j}\left(\frac{a}{b}, \theta\right) p_2 \sqrt{\pi a}, \quad i, j = 1, 2,$$
$$K_{iB_j} = F_{iB_j}\left(\frac{a}{b}, \delta\right) p_2 \sqrt{\pi b}, \quad i, j = 1, 2. \tag{31}$$

Figures 4(a) and 4(b) show the nondimensional SIF for an inclined crack when θ is changing for $\delta = 45^\circ$ and the nondimensional SIF for a curved crack when δ is changing for $\theta = 45^\circ$, respectively. It can be seen that as θ and δ vary within the range $0^\circ \le \delta \le 90^\circ$, the values of F_{1A_1}, F_{2A_1}, F_{1A_2}, F_{2A_2}, F_{1B_1}, F_{2B_1}, F_{1B_2}, and F_{2B_2} are varied significantly for the considered domain.

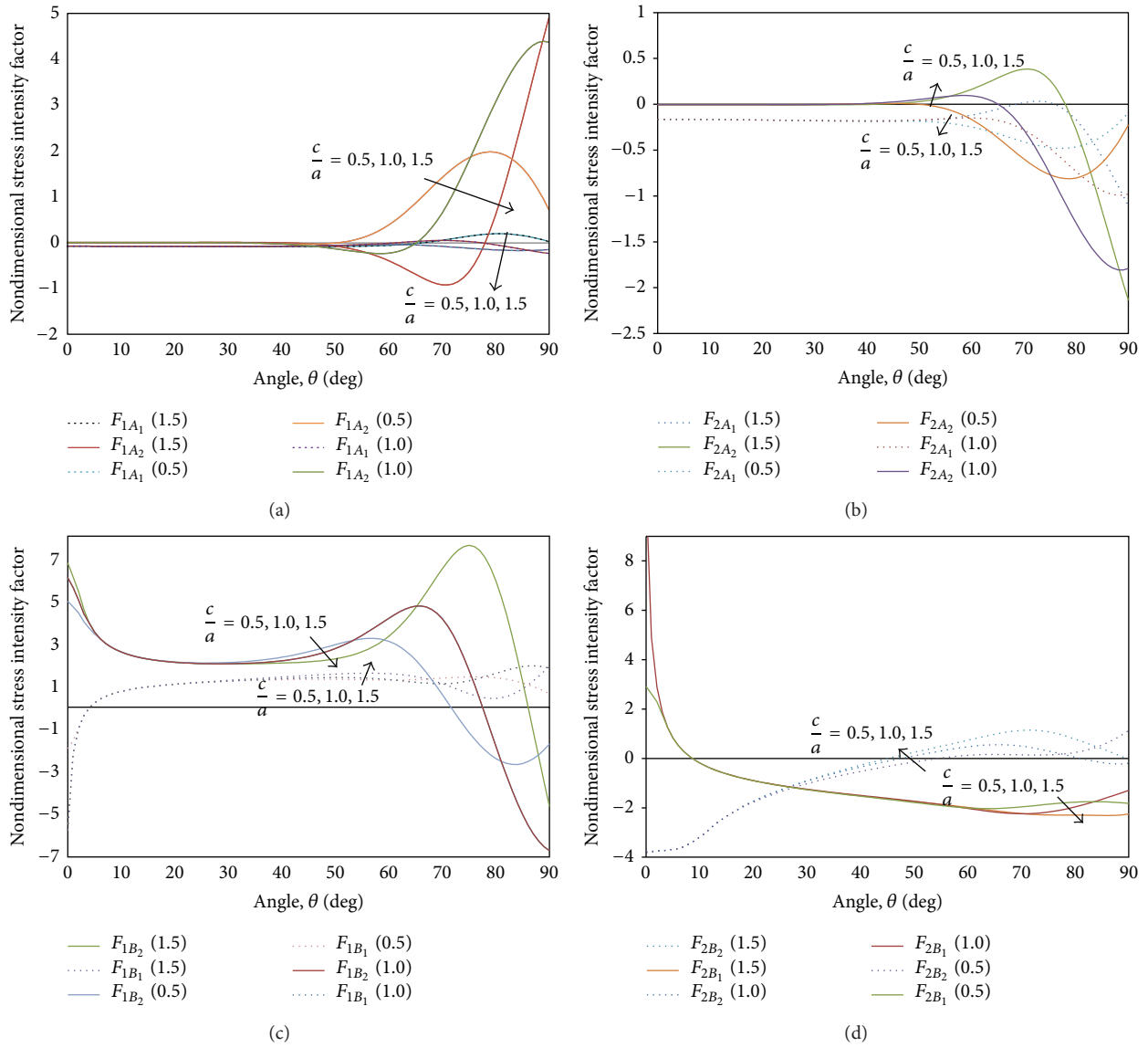

Figure 7: Nondimensional SIF at the crack tips when θ is changing subject to mix loading (see Figure 2(e)).

The effect of the distance between both cracks, a/b, is also studied by taking $\theta = 45^\circ$ and the results are shown in Figures 4(c) and 4(d) for $\delta = 90^\circ$ and $\delta = 45^\circ$, respectively. As the two cracks are close together, the nondimensional SIF at the crack tip becomes higher.

4.3. Example 3: Mode III. Consider the problem in Figure 2(c); the traction applied is $\sigma_{xy}^{\infty} = q$ and the calculated results for SIF at the crack tips A_1, A_2, B_1, and B_2 are, respectively, expressed as

$$K_{iA_j} = F_{iA_j}\left(\frac{a}{b}, \theta\right) q\sqrt{\pi a}, \quad i, j = 1, 2,$$
$$K_{iB_j} = F_{iB_j}\left(\frac{a}{b}, \delta\right) q\sqrt{\pi b}, \quad i, j = 1, 2. \tag{32}$$

Figures 5(a) and 5(b) show the nondimensional SIF for an inclined crack when θ is changing for $\delta = 45^\circ$ and the nondimensional SIF for a curved crack when δ is changing for $\theta = 45^\circ$, respectively. It can be seen that as θ and δ vary within the range $0^\circ \le \delta \le 90^\circ$, the values of F_{1A_1}, F_{2A_1}, F_{1A_2}, F_{2A_2}, F_{1B_1}, F_{2B_1}, F_{1B_2}, and F_{2B_2} are varied significantly for the considered domain.

The effect of the distance between both cracks, a/b, is also studied by taking $\theta = 45^\circ$ and the results are shown in Figures 5(c) and 5(d) for $\delta = 90^\circ$ and $\delta = 45^\circ$, respectively. As the two cracks are close together, the nondimensional SIF at the crack tip becomes higher.

4.4. Example 4: Mix Mode. Consider that the inclined crack is located at the lower position of the curved crack

(Figure 2(d)). The traction applied is $\sigma_y^\infty = \sigma_x^\infty = p$ and the calculated results for SIF at the crack tips A_1, A_2, B_1, and B_2 are, respectively, expressed as

$$K_{iA_j} = F_{iA_j}\left(\frac{c}{a}, \theta\right) p\sqrt{\pi a}, \quad i, j = 1, 2,$$
$$K_{iB_j} = F_{iB_j}\left(\frac{c}{a}, \theta\right) p\sqrt{\pi b}, \quad i, j = 1, 2. \tag{33}$$

Figures 6(a) and 6(b) show the interaction of both cracks by evaluating the nondimensional SIF at the crack tips A_1 and A_2 when $c/a = 1.5, 2.0, 2.5$ for F_1 and F_2, respectively, whereas Figures 6(c) and 6(d) show the interaction of both cracks by evaluating the nondimensional SIF at the crack tips B_1 and B_2 when $c/a = 1.5, 2.0, 2.5$ for F_1 and F_2, respectively. From these results, we see that F_1 and F_2 at the crack tip A_2 are higher than A_1.

4.5. Example 5. Consider that the inclined crack is located at the right position of the curved crack (Figure 2(e)). The traction applied is $\sigma_y^\infty = \sigma_x^\infty = p$ and the calculated results for SIF at the crack tips A_1, A_2, B_1, and B_2 are, respectively, expressed as

$$K_{iA_j} = F_{iA_j}\left(\frac{c}{a}, \theta\right) p\sqrt{\pi a}, \quad i, j = 1, 2,$$
$$K_{iB_j} = F_{iB_j}\left(\frac{c}{a}, \theta\right) p\sqrt{\pi b}, \quad i, j = 1, 2. \tag{34}$$

Figures 7(a) and 7(b) show the interaction of both cracks by evaluating the nondimensional SIF at the crack tips A_1 and A_2 when $c/a = 1.5, 2.0, 2.5$ for F_1 and F_2, respectively, whereas Figures 7(c) and 7(d) show the interaction of both cracks by evaluating the nondimensional SIF at the crack tips B_1 and B_2 when $c/a = 1.5, 2.0, 2.5$ for F_1 and F_2, respectively. As the c/a decreases, the nondimensional SIF becomes higher.

5. Conclusion

In this paper, the different types of loading modes have been applied to the inclined and curved cracks in plane elasticity. We obtained different results of nondimensional SIF due to the different loading modes. We also observed that the SIF increases as both cracks become closer.

Conflict of Interests

The authors declare that there is no conflict of interests regarding the publication of this paper.

Acknowledgment

The authors would like to thank the Ministry of Science, Technology and Innovation (MOSTI), Malaysia, for the Science Fund Vot no. 5450657.

References

[1] V. V. Panasyuk, M. P. Savruk, and A. P. Datsyshyn, "A general method of solution of two-dimensional problems in the theory of cracks," *Engineering Fracture Mechanics*, vol. 9, no. 2, pp. 481–497, 1977.

[2] B. Cotterell and J. R. Rice, "Slightly curved or kinked cracks," *International Journal of Fracture*, vol. 16, no. 2, pp. 155–169, 1980.

[3] I. Y. Shen, "Perturbation eigensolutions of elastic structures with cracks," *Transactions ASME, Journal of Applied Mechanics*, vol. 60, no. 2, pp. 438–442, 1993.

[4] P. A. Martin, "Perturbed cracks in two dimensions: an integral-equation approach," *International Journal of Fracture*, vol. 104, no. 3, pp. 317–327, 2000.

[5] Y. Z. Chen, N. Hasebe, and K. Y. Lee, *Multiple Crack Problems in Elasticity*, vol. 4, WIT Press, Southampton, UK, 2003.

[6] N. M. A. Nik Long and Z. K. Eshkuvatov, "Hypersingular integral equation for multiple curved cracks problem in plane elasticity," *International Journal of Solids and Structures*, vol. 46, no. 13, pp. 2611–2617, 2009.

[7] Y. Z. Chen, D. Gross, and Y. J. Huang, "Numerical solution of the curved crack problem by means of polynomial approximation of the dislocation distribution," *Engineering Fracture Mechanics*, vol. 39, no. 5, pp. 791–797, 1991.

[8] Y. Z. Chen, "A numerical solution technique of hypersingular integral equation for curved cracks," *Communications in Numerical Methods in Engineering*, vol. 19, no. 8, pp. 645–655, 2003.

[9] E. D. Leonel and W. S. Venturini, "Multiple random crack propagation using a boundary element formulation," *Engineering Fracture Mechanics*, vol. 78, no. 6, pp. 1077–1090, 2011.

[10] A. Portela, M. H. Aliabadi, and D. P. Rooke, "Dual boundary element analysis of cracked plates: singularity subtraction technique," *International Journal of Fracture*, vol. 55, no. 1, pp. 17–28, 1992.

[11] J. H. Guo and Z. X. Lu, "Anti-plane analysis of multiple cracks originating from a circular hole in a magnetoelectroelastic solid," *International Journal of Solids and Structures*, vol. 47, no. 14-15, pp. 1847–1856, 2010.

[12] N. I. Muskhelishvili, *Some Basic Problems of the Mathematical Theory of Elasticity*, Noordhoff International Publishing, Leyden, The Netherlands, 1957.

[13] K. Mayrhofer and F. D. Fischer, "Derivation of a new analytical solution for a general two-dimensional finite-part integral applicable in fracture mechanics," *International Journal for Numerical Methods in Engineering*, vol. 33, no. 5, pp. 1027–1047, 1992.